JOURNAL OF PROPULSION AND POWER
Vol. 26, No. 2, March–April 2010

Ignition Delay Time Measurements of Normal Alkanes and Simple Oxygenates

D. F. Davidson,* S. C. Ranganath,* K.-Y. Lam,* M. Liaw,* Z. Hong,* and R. K. Hanson*
Stanford University, Stanford, California 94305

DOI: 10.2514/1.44034

Ignition delay time data for higher *n*-alkanes are required for the development and refinement of jet fuel surrogate mechanisms; similar data for oxygen-carrying species are also required for the development of oxygenate fuel mechanisms. To fill this need, ignition delay times were measured using pressure and OH* emission diagnostics behind reflected shock waves for a series of higher *n*-alkanes and for several simple oxygenates. Reflected shock conditions covered temperatures of 1150–1550 K and pressures of 1–4 atm (0.1–0.4 MPa). Fuel mixtures tested include the four *n*-alkanes: *n*-pentane, *n*-hexane, *n*-octane, and *n*-nonane; and the four oxygenates: acetone, *n*-butanal, methyl butanoate, and 3-pentanone. All fuels were tested in oxygen/argon mixtures with equivalence ratios of 0.5 to 2.0. The ignition data were compared with current models and a new *n*-butanal reaction mechanism, based on previous studies, was used to model the *n*-butanal and methyl butanoate data.

Introduction

THE development and refinement of reaction mechanisms for combustion processes requires an extensive database of kinetic targets and chemical reaction rates. Shock tube experiments can provide data for this purpose, including reaction rate constants, species time histories, and ignition delay times [1]. Ignition delay times, in particular, provide the simplest overall performance characteristic of a combustion system [2]. When measured in a shock tube, they can often be simply modeled as a constant volume reactor system with well-defined temperatures, pressures, mixture concentration, and effectively instantaneous temperature jump.

Jet fuel surrogate mechanisms often use normal alkanes to represent the bulk of the many individual fuel constituents found in distillate jet fuels, such as JP-8 (used by the military) and its commercial equivalent Jet-A. The recent development of an *n*-alkane jet fuel surrogate mechanism JetSurF by Sirjean et al. is based on a hierarchal structure that includes species and reactions for all *n*-alkanes up to *n*-dodecane [3]. Initial testing and refinement of this mechanism used existing ignition delay time data for several *n*-alkanes (e.g., *n*-heptane and *n*-dodecane). However, a high-temperature data set for an extended series of *n*-alkanes (C_5 and higher) taken under similar conditions is also needed. Similar model development work by Westbrook et al. at Lawrence Livermore National Laboratory on a mechanism for *n*-alkanes up to *n*-hexadecane has suggested that, at higher temperatures (above the NTC regime), only small variations in ignition delay times are expected among all *n*-alkane fuel surrogates with C_4 and higher [4].

Parallel to the jet fuel mechanism development, efforts are being made to understand the influence of oxygenate additives on distillate fuel performance, as well as the potential use of neat oxygenates as fuels themselves. The addition of oxygenates to distillate fuels has been demonstrated to reduce emissions, and pure oxygenate fuels (e.g., biodiesels), which are composed primarily of methyl esters, have also been demonstrated to produce reduced emissions. Surveys of ignition delay time are needed to develop and test oxygenate reaction mechanisms and to understand how their behavior changes with oxygenate type; little ignition delay data suitable for oxygenate-to-oxygenate comparisons exist. As well, we have found only a limited number of studies that develop oxygenate reaction mechanisms; in particular, we have not found published reaction mechanisms for two larger oxygenates: butanal and 3-pentanone {but, see Herbinet et al. for the recent development of a reaction mechanism for methyl decanoate [5]}.

In this study, we present ignition delay time data for a series of higher *n*-alkanes: *n*-pentane, *n*-hexane, *n*-octane, and *n*-nonane; and a set of simple oxygenates: acetone, *n*-butanal, methyl butanoate (MB), and 3-pentanone. For several of these fuels, *n*-nonane, *n*-butanal, and 3-pentanone, we believe these data represent the first published ignition delay time measurements. These *n*-alkane data are also compared with simulations using current mechanisms and correlations. For butanal, for which no current mechanism exists, we have developed a small modification to the MB reaction mechanism of Dooley et al. that satisfactorily describes the ignition behavior of both the C_4 aldehyde and MB [6]. These measurements are part of a continuing program in our laboratory to develop a fundamental kinetic database using shock tubes [1].

Experimental Method

Ignition delay time measurements of oxygenates and straight-chain alkanes were obtained behind reflected shock waves in a high-purity low-pressure kinetics shock tube regularly used in our laboratory. The stainless steel shock tube is composed of a 3.35 m driver section and an 8.54 m driven section with both sections 14.13 cm in inner diameter. Shock waves are produced by over-pressuring thin polycarbonate diaphragm (of thickness 0.12–0.25 mm) until rupture with high-pressure helium. Incident shock speeds were measured over the last 1.5 m of the driven section using five PCB model 113 pressure transducers (PZT) and four Phillips/Fluke model PM5555 interval counters, and these values were extrapolated to the endwall location. Shocked gas conditions were calculated using a conventional chemically frozen shock equation solver and confirmed using a Kistler model 603B1 PZT located 20 mm from the shock tube endwall; initial reflected shock temperatures and pressures spanned 1150–1550 K and 1–20 atm (0.1–2 MPa), respectively. Because of the short measured ignition delay times and the large diameter of the shock tube used in these experiments, we do not anticipate any significant effect on the test conditions from the reflected shock wall bifurcation. The shock tube and optical diagnostics arrangement are shown in Fig. 1.

Ignition events were determined by observing OH* emission near 306 nm through UV-grade fused silica windows in the shock tube end section. Two OH* emission diagnostics consisting of Thorlabs model PDA 34 silicon photodetectors, collimating optics, and slits and Schott glass UG-5 filters were located at the endwall and at a

Received 25 February 2009; revision received 14 October 2009; accepted for publication 24 November 2009.

*Department of Mechanical Engineering.

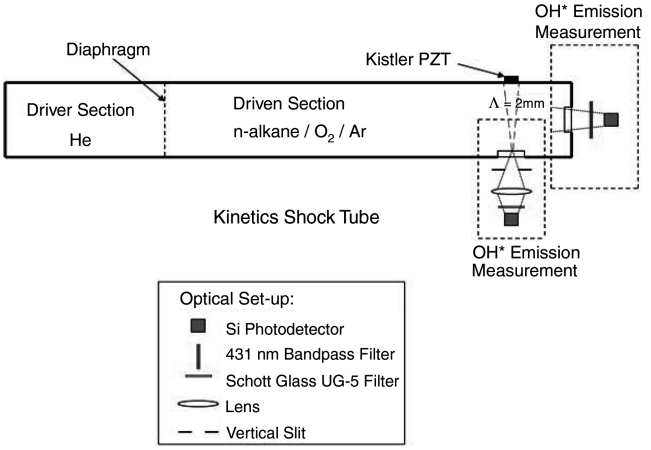

Fig. 1 Kinetics shock tube schematic and optical diagnostic arrangement.

sidewall position 20 mm upstream from the endwall. In the acetone ignition delay time experiments, labeled side in Table 2, OH* and CH* emission diagnostics were used, both at the sidewall location; in the MB experiments only, the OH* sidewall emission diagnostic was used.

Test gas mixtures were prepared beforehand in a heated, stainless steel, turbomolecular pumped, 22 liter mixing tank with a magnetically driven stirring fan. For *n*-octane and *n*-nonane mixtures, which have low room-temperature vapor pressures, the mixing tank and manifold were heated to 70°C; all other mixtures were made at room temperature. Research-grade argon and O_2 from Praxair were used in all mixtures, along with 99.5 + % pure fuels from Sigma–Aldrich that were degassed by vacuum pumping before use.

Ignition Delay Time Measurements and Discussion

Ignition delay times can be inferred in one of three ways in these shock tube experiments: using sidewall pressure or sidewall or endwall emission. Representative data traces for three of the fuels are shown in Figs. 2–4. In all the experiments presented here, endwall emission or sidewall emission measurements were used to determine the ignition delay time. The pressure measurement, although registering some increase in value during ignition, does not give an unequivocal ignition time, as the energy release (and coincident pressure rise) is gradual and continuous (often starting significantly before the rapid formation of radicals that the emission measurement captures) for the low fuel concentrations used in these experiments.

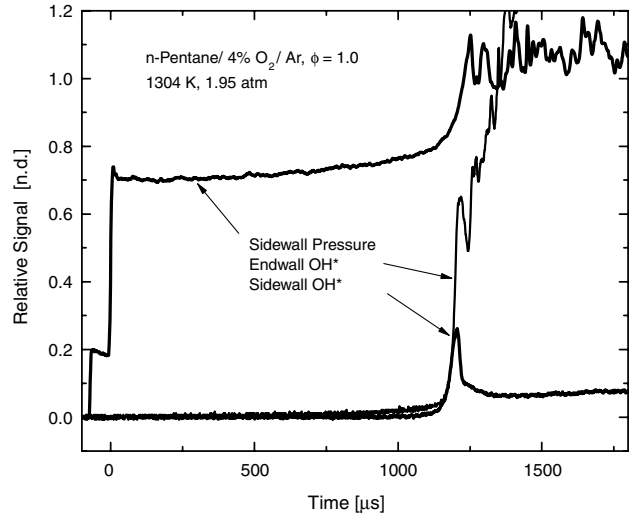

Fig. 2 Example ignition delay time measurement in *n*-pentane. Initial mixture: 0.5% *n*-pentane, 4% O_2, balance argon (n.d. denotes no dimension).

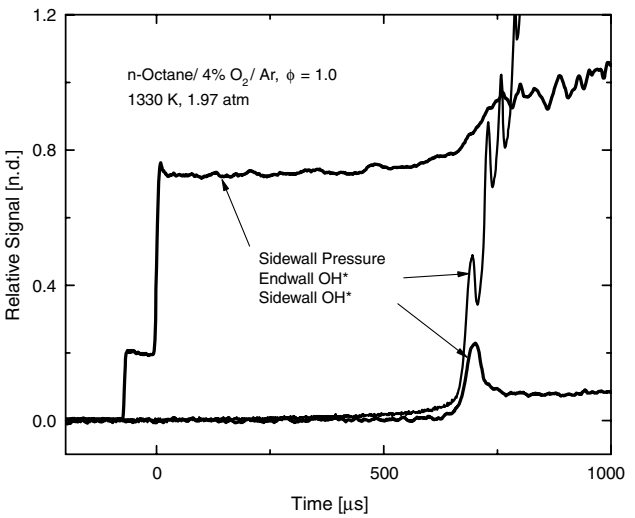

Fig. 3 Example ignition delay time measurement in *n*-octane. Initial mixture: 0.32% *n*-octane, 4% O_2, balance argon.

For the endwall emission measurements, the ignition delay time of the mixture was defined as the time interval between the arrival of the incident shock at the endwall of the shock tube (calculated using the incident shock velocity and the arrival time at the sidewall-mounted pressure transducer) and the extrapolation of the maximum slope of the endwall OH* emission trace to the zero signal level. Overall uncertainty in the ignition delay time measurements is ±10%; this must be convoluted with the ±1% uncertain in temperature.

In the sidewall emission measurements (used to confirm the endwall measurements when they both were acquired), the ignition delay time was defined as the time interval between the arrival of the reflected shock at the sidewall observation (location 2 cm from the endwall) and the extrapolation of the maximum slope of the OH* sidewall emission trace to the zero signal level. See Fig. 4 for an example determination. Because the ignition of the test gas mixture at the endwall location occurs first, this test gas volume can expand and perturb gas volumes further away from the endwall. This effect can shorten the observed sidewall ignition time measurement when compared with the endwall measurement, typically by an amount of 5–40 μs. This effect can be significant at higher temperatures, at which ignition delay times are shorter than 200 μs, but can usually be ignored for longer ignition delay times.

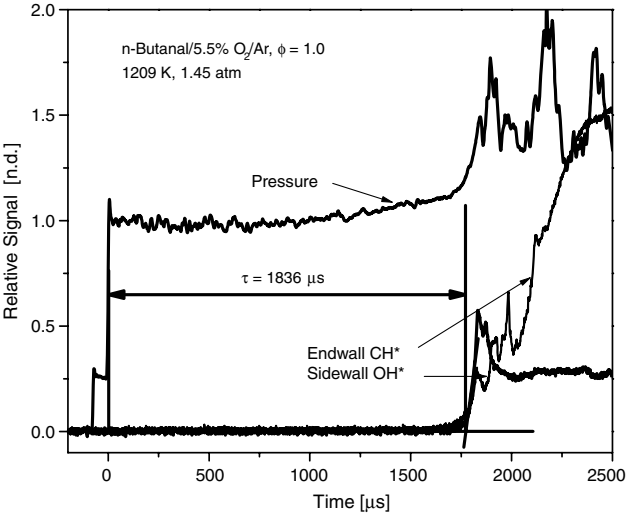

Fig. 4 Example ignition delay time measurement in *n*-butanal. The sidewall ignition delay time for this experiment (1836 μs) is indicated. Initial mixture: 0.727% *n*-butanal, 4% O_2, balance argon (corresponding to $\phi = 1$).

Table 1 Ignition delay times for *n*-alkane

P_5, atm	T_5, K	Endwall ignition time, μs	P_5, atm	T_5, K	Endwall ignition time, μs
	n-pentane, $\phi = 1.0$, 4% O_2/Ar			*n*-nonane, $\phi = 1.0$, 4% O_2/Ar	
1.74	1489	145	1.85	1307	1002
1.83	1426	281	1.68	1288	1351
1.91	1360	603	1.80	1384	382
1.95	1304	1227	1.86	1367	499
2.00	1267	1845	1.91	1330	780
3.61	1303	832	3.63	1348	405
3.75	1261	1455	3.46	1263	1237
3.47	1395	316	3.58	1372	318
3.41	1449	162	3.45	1359	349
3.61	1268	1296		*n*-pentane, $\phi = 0.5$, 4% O_2/Ar	
	n-hexane, $\phi = 1.0$, 4% O_2/Ar		1.65	1396	255
1.92	1284	1317	1.73	1263	1391
1.90	1353	623	1.71	1533	49
1.76	1358	688	1.62	1428	153
1.77	1470	176	1.75	1397	232
1.86	1375	483		*n*-hexane, $\phi = 0.5$, 4% O_2/Ar	
1.93	1237	2706	1.77	1475	78
3.32	1273	1046	1.76	1274	1225
3.60	1396	301	1.89	1361	303
3.10	1250	1805	1.67	1367	308
3.48	1386	291	1.69	1403	196
3.43	1407	263		*n*-octane, $\phi = 0.5$, 4% O_2/Ar	
	n-octane, $\phi = 1.0$, 4% O_2/Ar		1.91	1434	104
1.95	1325	859	1.98	1307	663
2.05	1265	1569	2.07	1273	988
2.01	1289	1198	2.19	1252	1269
1.96	1385	390	2.01	1380	220
1.87	1455	166		*n*-nonane, $\phi = 0.5$, 4% O_2/Ar	
3.37	1282	1020	1.67	1403	190
3.59	1421	210	1.78	1399	180
3.63	1384	285	1.75	1331	421
3.75	1319	614	1.87	1350	317
3.81	1273	1064	1.81	1299	730
			1.92	1305	536
			1.96	1284	781
			1.84	1385	231
			1.82	1470	93

In Figs. 2–4, after ignition, there is evidence of large oscillations in the pressure trace (and the endwall emission measurement) resulting from the formation of a blast wave. These oscillations are not seen in the sidewall emission data, as the sidewall emission diagnostic sees only the small volume adjacent to the window, whereas the endwall emission diagnostic continues to view the entire length of the shock tube driven section.

Ignition Delay Time Data for *n*-Alkane

Normal alkane ignition delay time data are presented in Table 1 and shown in Arrhenius form in Figs. 5 and 6.

As predicted by Westbrook et al. [4] and others, only small differences are seen in the ignition delay time data for these four *n*-alkanes at the temperatures studied. A small systematic decrease (15%) in ignition delay time is seen between the two carbon number extremes (C_5 and C_9). This systematic decrease in ignition delay time, or increase in reactivity of the fuel, is related to the decrease in average C–H bond strength (bond dissociation energy). Larger alkanes have higher ratios of secondary to primary C–H bonds, and secondary C–H bonds have lower bond strengths than primary C–H bonds. Activation energies over the temperature range studied fall randomly between 42 and 44 kcal/mol for each of the *n*-alkane $\phi = 1$ mixtures. For the alkane $\phi = 0.5$ mixtures, they are slightly higher, falling between 46 and 52 kcal/mol. The small number of measurements prevents any further discernment of systematic behavior in the activation energy.

All of the 4% oxygen/argon *n*-alkane data were least-squares correlated in the form:

$$\ell n(\tau_{\text{ign}}) = \ell n(A) + N\,\ell n(P) + M\,\ell n(C_\#) + S\,\ell n(\phi) + \mathrm{E}_A/RT$$

with τ_{ign} in μs, P in atm, T in K, and E_A in cal/mol, with the result that

$$\tau_{\text{ign}} = 7.83 \times 10^{-5} P^{-0.53} C_\#^{-0.24} \phi^{0.80} \exp(44,770/RT)[\mu\text{s}]$$

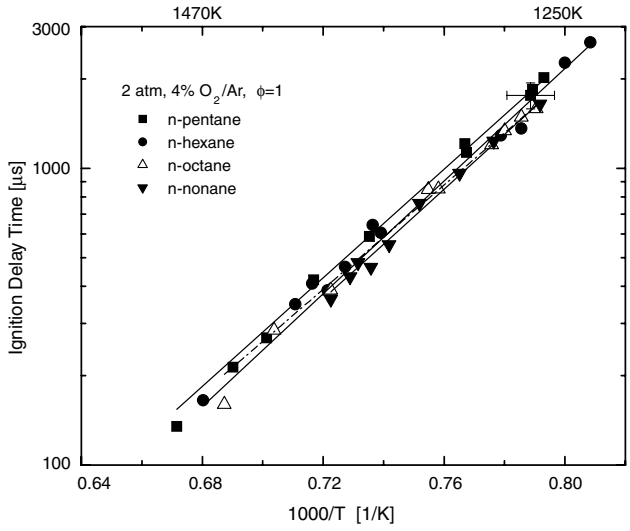

Fig. 5 Arrhenius plot of *n*-alkane ignition delay times, $\phi = 1$. Data in this figure and Fig. 6, covering pressures from 1.7 to 3.8 atm (0.17–0.38 MPa), were normalized to 2 atm (0.2 MPa) using an overall correlation pressure dependence of $P^{-0.52}$. Representative ±10% ignition delay time error bars and ±1% temperature error bars are shown for one point.

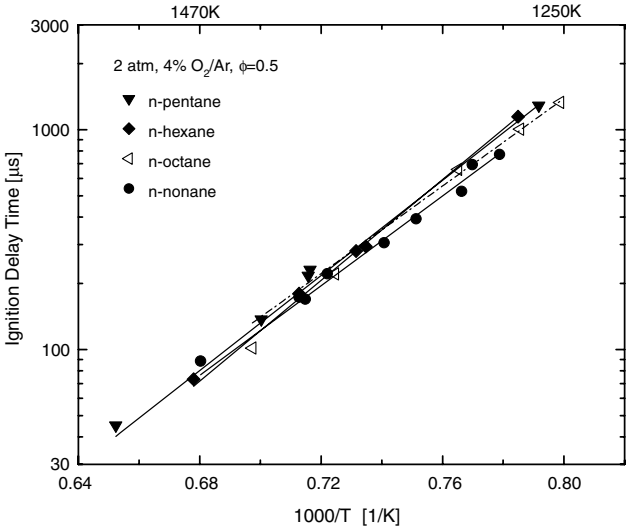

Fig. 6 Arrhenius plot of *n*-alkane ignition delay times [$\phi = 0.5$, 4% oxygen/argon, 2 atm (0.2 MPa)].

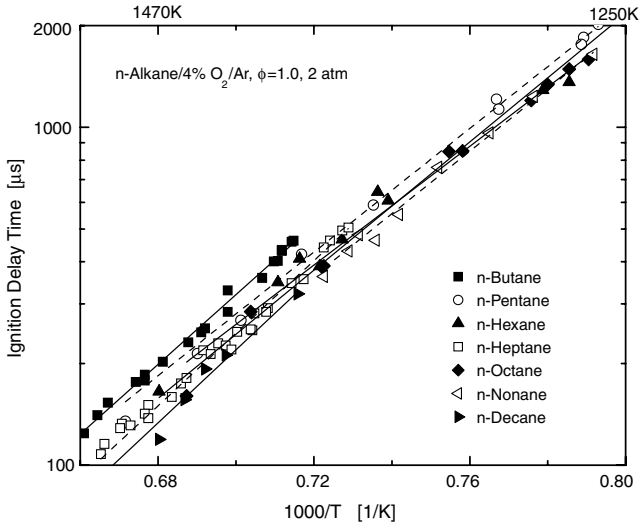

Fig. 7 Arrhenius plot of *n*-alkane ignition delay times for $\phi = 1$ from the present study and that of Horning et al. [7].

Limited to just the $\phi = 1$ *n*-alkane data, the correlation is

$$\tau_{\text{ign}} = 1.78 \times 10^{-4} P^{-0.52} C_{\#}^{-0.26} \exp(42,620/RT)[\mu\text{s}]$$

R-squared values for both correlations exceed 0.99. Ignition delay time data presented in all figures were normalized using an inverse pressure scaling.

These results can be compared with the previous measurements of Horning et al. [7] (from our laboratory) that overlap with the present experimental conditions. Those authors found that for stoichiometric mixtures ($\phi = 1$) of the four *n*-alkanes (propane, butane, heptane, and decane),

$$\tau_{\text{ign}} = 9.4 \times 10^{-6} P^{-0.55} X_{\text{O2}}^{-0.63} C_{\#}^{-0.50} \exp(46,550/RT)[\mu\text{s}]$$

The pressure dependence of the current study and that of Horning et al. [7] are very close, but the dependencies on carbon number are different; the activation energies are similar but statistically different. The data from the present study, along with the data from Horning et al. at (or near) $\phi = 1$ and $X_{\text{O2}} = 4\%$, were correlated together (representing a total of 97 data points: 57 from Horning et al. and 40 from the current study, covering the full series of the *n*-alkanes range, from *n*-butane to *n*-decane, completely). In this correlation, the ignition delay time was found to be

$$\tau_{\text{ign}} = 1.75 \times 10^{-4} P^{-0.54} C_{\#}^{-0.39} \exp(43,410/RT)[\mu\text{s}]$$

Figure 7 shows the complete series of *n*-alkane ignition delay time measurements from the present study and from Horning et al. [7]. Scatter in these measurements is small enough that the systematic variation in ignition delay time from C_4 (*n*-butane) to C_{10} (*n*-decane) is evident.

Oxygenate Ignition Delay Time Data

Oxygenate ignition delay time data are presented in Tables 2 and 3 and shown in Arrhenius form in Figs. 8 and 9. The data taken over the range of pressures 1.4–2.8 atm (0.14–0.28 MPa) were normalized to 1.7 atm (0.17 MPa) using the pressure scaling found for the *n*-alkanes: $\tau_{\text{ign}} \sim P^{-0.52}$. This pressure scaling also predicts the

Table 2 Oxygenate ignition delay times

P_5, atm	T_5, K	Endwall ignition time, μs	P_5, atm	T_5, K	Endwall ignition time, μs
3-pentanone, 4% O_2/Ar, $\phi = 1.0$			*n*-butanal, 5.5% O_2/Ar, $\phi = 1.0$		
1.68	1306	280	1.41	1397	156
1.73	1259	545	1.40	1296	580
1.77	1209	1022	1.37	1423	107
1.80	1188	1337	1.45	1236	1292
1.85	1173	1626	1.48	1308	454
MB, 4% O_2/Ar, $\phi = 1.0$, side			1.45	1209	1836
1.77	1299	898	2.68	1264	598
1.71	1358	440	2.77	1188	1589
1.67	1385	306	2.51	1352	196
1.80	1244	2036	2.73	1229	1023
1.74	1323	703	2.62	1318	306
1.73	1282	1089	2.51	1388	135
1.70	1353	433	*n*-butanal, 2.75% O_2/Ar, $\phi = 2.0$		
1.65	1373	307	1.46	1352	1034
1.69	1446	132	1.39	1411	602
1.74	1262	1778	1.37	1506	237
1.76	1330	607	1.34	1551	158
MB, 4% O_2/Ar, $\phi = 0.5$, side			1.47	1296	1610
1.70	1403	153	*n*-butanal, 4% O_2/Ar, $\phi = 1.0$		
1.72	1326	491	1.78	1248	1188
1.80	1287	926	1.75	1306	534
1.84	1238	1903	1.80	1195	2452
1.81	1264	1200	1.81	1234	1451
1.77	1308	706			

Table 3 Acetone ignition delay times

P_5, atm	T_5, K	Endwall ignition time, μs	P_5, atm	T_5, K	Endwall ignition time, μs
Acetone, 4% O_2/Ar, $\phi = 1.0$			Acetone, 4% O_2/Ar, $\phi = 2.0$, side		
1.38	1417	456	1.55	1443	553
1.30	1471	242	1.50	1475	403
1.30	1540	115	1.55	1359	1317
1.45	1322	1548	1.62	1327	1856
1.46	1373	885	1.63	1548	171
Acetone, 4% O_2/Ar, $\phi = 1.0$, side			1.48	1269	4105
1.53	1230	5114	1.53	1310	2791
1.50	1249	4220	1.66	1500	292
1.44	1292	2557	1.46	1256	4548
1.53	1329	1394	1.51	1374	1138
1.50	1363	966	1.49	1466	453
1.57	1411	531	1.70	1585	122
1.53	1447	321			
1.55	1496	178			
1.50	1506	150			
21.1	1169	2580			
20.3	1181	2166			
19.7	1240	1101			
19.4	1276	707			
18.5	1285	632			

behavior of the limited number of 20 atm (2.0 MPa) acetone experiments conducted as part of this study.

The magnitudes of the ignition delay times of the oxygenates studied decreases as the total carbon number increases. This variation in carbon number is clearly evident within the ketone class, for which the ignition delay time for 3-pentanone is one-sixth of that for acetone. Also of note is that the ignition delay times for 3-pentanone are one-fifth of the values for *n*-pentane and at similar conditions, indicating that the chemistry controlling the ignition process of 3-pentanone must differ significantly in certain aspects from that of the normal alkanes.

Activation energies of the ignition delay time measurements for 3-pentanone, acetone, and butanal are similar ($E_A \sim 43$ kcal/mol) for the experiments performed at temperatures less than ~1350 K. This activation energy is similar to that found for *n*-alkanes in this study (the fit to the *n*-pentane data is also shown in Fig. 8), indicating that, although the chemistry controlling the magnitude of the ignition delay times of oxygenates is different than that of normal alkanes, the chemistry controlling the ignition delay time activation energy must be similar. At higher temperatures in acetone (for both $\phi = 1$ and 2) and at all temperatures measured for MB, the activation energy is slightly higher ($E_A \sim 50$ kcal/mol). This higher activation energy is also seen in the more oxygen-rich $\phi = 0.5$ *n*-alkane data, possibly indicating that there is a similar increase in oxygen-carrying radicals in the oxygenate systems that exhibit this higher activation energy behavior.

Measurements of ignition delay time for acetone mixtures were also performed by Sato and Hidaka [8] (shown in Fig. 9) and Pichon et al. [9]. Good agreement is seen with the measurements of Sato and Hidaka [8], who used the same mixtures as the present study at a slightly higher pressure (1.9–2.8 atm, 0.19–0.28 MPa) when their data were normalized to 1.7 atm (0.17 MPa) (using $P^{-0.52}$).

Model Comparison

Preliminary comparisons were performed between the measured ignition delay times and simulations based on several recently developed mechanisms.

n-Alkanes

Figures 10 and 11 present a comparison of simulations employing a preliminary version of the JetSurF mechanism (Sirjean et al. [3]) with the *n*-alkane ignition delay time data. This mechanism was designed to simulate the high-temperature jet engine chemistry of the

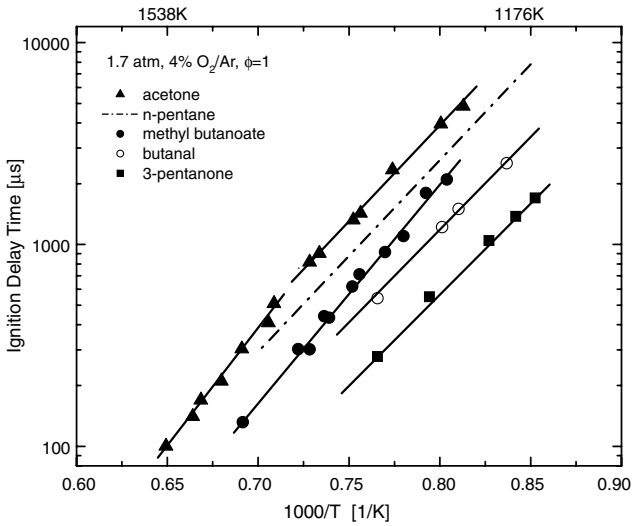

Fig. 8 Arrhenius plot of oxygenate species ignition delay times, $\phi = 1.0$. The dot-dashed line is the fit through the current *n*-pentane ignition delay time measurements.

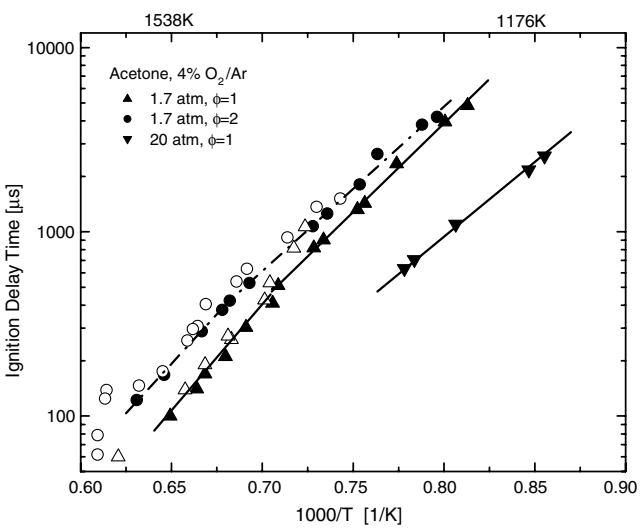

Fig. 9 Arrhenius plot of acetone ignition delay times at two equivalence ratios and two pressures: current study (solid symbols) and measurements of Sato and Hidaka [8] at similar conditions (open symbols).

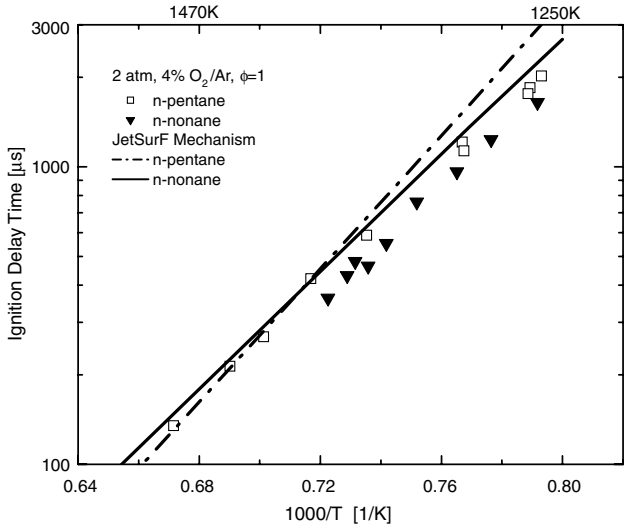

Fig. 10 Comparison of experiment and simulation (JetSurF/Sirjean et al. [3]) for *n*-alkane ignition delay times [$\phi = 1.0$, 4% oxygen/argon, 2 atm (0.2 MPa)].

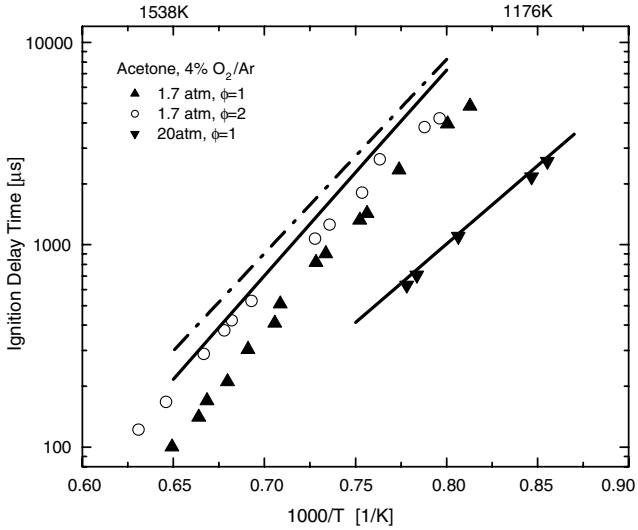

Fig. 12 Comparison of experiment and model (Pichon et al. [9]) for acetone ignition delay times for two equivalence ratios and two pressures: modeled values for $\phi = 1$ (solid lines) and $\phi = 2$ (dot-dashed line).

single-component jet fuel surrogate *n*-dodecane and, in doing so, was based on a hierarchy of lower *n*-alkanes. Agreement with the results of the lower *n*-alkanes is satisfactory. The tight grouping of the ignition delay times of the *n*-alkanes found in the present measurements is duplicated in the modeled results for both the $\phi = 0.5$ and 1.0 data. Small variations in activation energy are seen for individual alkanes (E_A for *n*-pentane is slightly higher than the measured value, for example.) Further refinement of this mechanism using shock tube data is possible through comparisons with species concentration time histories and by use of directly determined individual reaction rates.

Ketones

Figure 12 presents a comparison of the recent Pichon et al reaction mechanism for acetone [9] with the measured acetone ignition delay time data. There is excellent agreement between the modeled and experimental activation energies, including the subtle change in activation energy with the equivalence ratio ϕ. The slight convergence of the $\phi = 1$ and 2 data at lower temperatures (near 1250 K) is seen in both the model and the 1.7 atm (0.17 MPa) data. The magnitudes of the modeled ignition delay times are about 50% greater than those measured at 1.7 atm (0.17 MPa), but they are in complete agreement at 20 atm (2.0 MPa). Pichon et al. used species profiles in flames, in addition to ignition delay times, to refine their mechanism. Again, once available, shock tube species concentration time history data will allow for further refinement of the mechanism.

We have not found a published reaction mechanism with which to compare the 3-pentanone ignition delay time measurements. However, it should be noted that, although the structure of the two ketones (acetone and 3-pentanone) are similar (they both have identical alkyl radicals on each side of the carbonyl group), their ignition delay times differ significantly. The ignition delay time for acetone CH_3COCH_3 is seven times that of 3-pentanone $C_2H_5COC_2H_5$. The possible role of higher ketones as fuel tracers in combustion systems [10,11] will require more detailed information about their oxidation and decomposition chemistry if we are to understand the influence of ketones as additives on ignition processes. In particular, differences in species lifetimes at high temperatures as a function of structure (e.g., 2-pentanone $CH_3COC_3H_7$ vs 3-pentanone) are important and cannot yet be predicted reliably.

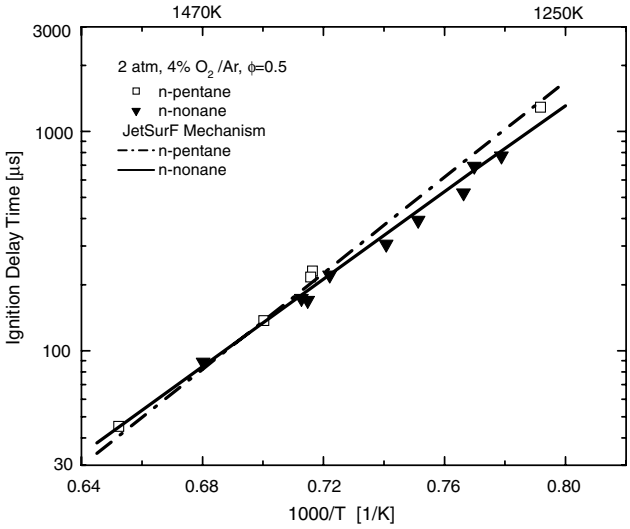

Fig. 11 Comparison of experiment and simulation (JetSurF/Sirjean et al. [3]) for *n*-alkane ignition delay times [$\phi = 0.5$, 4% oxygen/argon, 2 atm (0.2 MPa)].

Larger Oxygenates

Figure 13 presents a comparison of the MB $C_3H_7CO_2CH_3$ and *n*-butanal C_3H_7CHO ignition delay time measurements with the Dooley et al. MB mechanism [6].

For the *n*-butanal modeling, the Dooley et al. [6] mechanism was slightly modified by the addition of two *n*-butanal decomposition reactions. The Dooley et al. mechanism already included a significant set of *n*-butanal and radical reactions but not the decomposition reactions that were expected to be important in high-temperature decomposition and ignition chemistry. These two added reactions and their estimated reaction rate constants[†] are

Reaction 1:

$$C_3H_7CHO \rightarrow C_2H_5 + CH_2CHO$$

Reaction 2:

$$C_3H_7CHO \rightarrow nC_3H_7 + HCO$$

$$k_1 = k_2 = 3 \cdot 10^{16} \exp(-82,000/RT)\,[s^{-1}] \quad (1)$$

The Dooley et al. [6] mechanism recovers the activation energy of the MB, and the modified Dooley et al. mechanism approximates the *n*-butanal ignition delay times. However, the MB model predicts 50%

[†]D. M. Golden, personal communication, Stanford University, 2008.

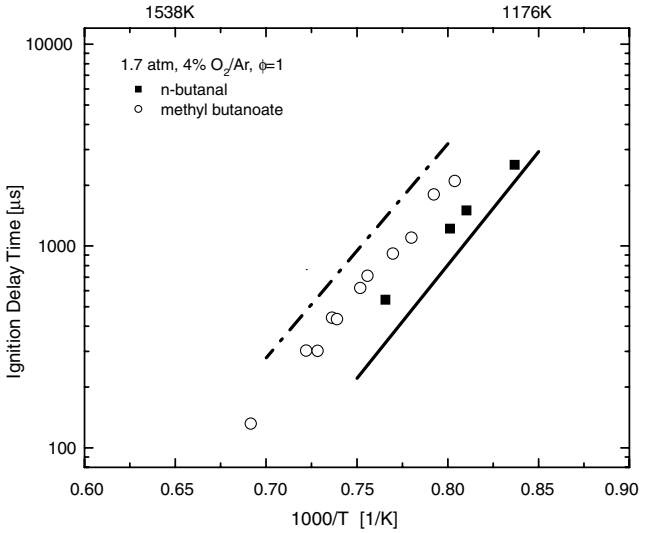

Fig. 13 Comparison of current MB ignition delay time data with model by Dooley et al. [6] (open symbols and dot-dashed line) and current *n*-butanal data with the modified model of Dooley et al. (solid symbols and lines.)

longer ignition delay times, and the (modified) *n*-butanal model predicts 25% shorter ignition delay times than measured.

These results can be related to the previous ketone measurements. Both MB and *n*-butanal have identical C_3H_7 subgroups on one side of their carbonyl carbon, but they have different subgroups ($-OCH_3$ and $-H$) on the opposite side. Their ignition delay times, however, are within 60% of each other. Although not measured in the study, 2-pentanone has the similar C_3H_7 subgroup with an opposing CH_3 subgroup. The 2-pentanone ignition delay time may be similar to that of MB and *n*-butanal, or it may be similar to acetone, which has CH_3 on both sides of the carbonyl group.

Some understanding of the mechanistic differences between *n*-butanal and MB can be gained by examining the major species profiles. Oxygen/fuel mole fraction ratios for these two fuels are similar for equivalence ratios (ϕ) of 1 ($X_{O2}/X_{butanal} = 5.5$; $X_{O2}/X_{MB} = 6.5$). Figures 14 and 15 show calculated species profiles for the major hydrocarbon species during the ignition of these two fuels at two differing temperatures but for cases for which the ignition delay times are similar. Several observations can be made.

The early time plateau level of the OH radical, which is an indicator of the small radical pool population, is predicted to be significantly smaller (5 ppm) for MB than for *n*-butanal (15 ppm). However, the oxygen-carrying species CH_2O and CH_2CO are

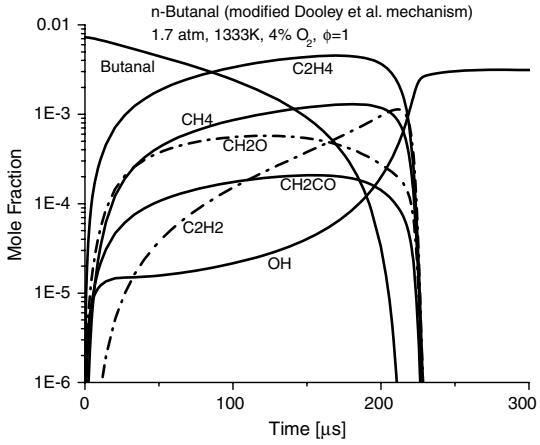

Fig. 14 Calculated species time histories for *n*-butanal ignition, using the modified Dooley et al. mechanism [6].

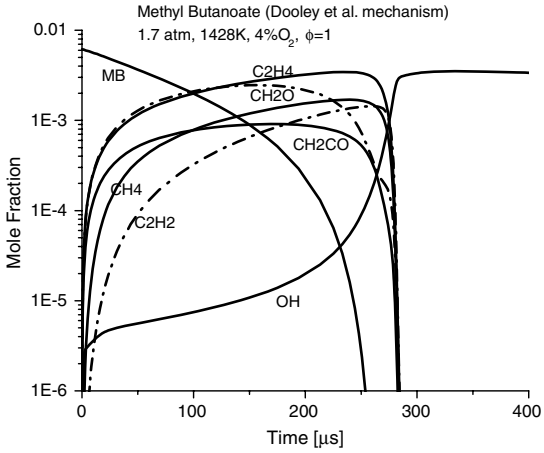

Fig. 15 Calculated species time histories for MB ignition, using the Dooley et al. mechanism [6].

approximately three to five times larger in the MB calculation when compared with their concentration in the *n*-butanal calculation. Stable hydrocarbon species, such as C_2H_4 and CH_4, are formed in different concentration ratios in both systems and have different overall magnitudes. The plateau levels of these stable intermediates are directly influenced by the oxygenate decomposition pathways proposed in their respective mechanisms. Shock tube measurements of OH concentration time histories using laser absorption would allow one to test the model predictions concerning oxidation pathways of these fuels. As well, measurements of the stable hydrocarbon intermediates (C_2H_4 and CH_4), using infrared laser absorption methods, would allow testing and validation of the proposed oxygenate decomposition pathways.

Conclusions

Ignition time data were obtained for a series of *n*-alkanes (C_5 to C_9), and comparisons with JetSurF [3], a current jet fuel surrogate mechanism, were made. The current measurements and those of Horning et al. [7], which cover a different subset of *n*-alkanes at similar conditions, are in close agreement. Most importantly, these two sets of experiments (both conducted in the same laboratory) confirm that the low-pressure (~2 atm, 0.2 MPa), high-temperature (greater than 1250 K) ignition delay times of higher *n*-alkanes (C_4 to C_{10}) are only weakly dependent on carbon number.

Ignition delay times were also measured for a series of oxygenate species and compared with simulations. A preliminary kinetic model for *n*-butanal ignition was developed based on the Dooley et al. [6] MB mechanism, and it successfully predicts the trends of the *n*-butanal ignition time data. This work identifies the continuing need for experimental data on large oxygenate molecules and, in particular, the systematic study of the influence of structural subgroups on ignition time behavior as important.

Future work will involve extending the *n*-alkane ignition delay time database to lower temperatures and higher pressures [negative temperature coefficient (NTC) regime], at which a different systematic behavior of ignition time with carbon number is predicted to occur. Currently, only limited data at these conditions exist for *n*-heptane, *n*-decane, and *n*-dodecane. Future work will also extend the investigation of oxygenate decomposition and ignition chemistry and include a study of the effect of different ligand structures near a carbonyl subgroup. Laser absorption measurements of key species (e.g., OH, CO_2, C_2H_4, and CH_4) will allow testing and validation of the predicted decomposition pathways in these oxygenate mechanisms. Some work in this area has begun because of the importance of these species (methyl esters) as a chemically simple surrogate for biodiesel fuels. A recent laser absorption/shock tube study in our laboratory found that predicted decomposition pathways for MB were not consistent with the CO_2 yields measured during

decomposition [12]. Further work is needed to improve these mechanisms.

Acknowledgments

This work was supported by the Army Research Office through grant number W911NF-07-1-0084 with Ralph Anthenien as contract monitor, by the Air Force Office of Scientific Research through grant number FA9550-08-1-0040 (Air Force Research Laboratory, Energy Integrated Product Team Program) with Julian Tishkoff as contract monitor, and by the Department of Energy through grant number De-FG02-88ER-13857 with Wade Sisk as contract monitor. The authors would also like to thank David M. Golden of Stanford University for his comments about butanal chemistry.

References

[1] Davidson, D. F., and Hanson, R. K., "*Fundamental Kinetics Database Utilizing Shock Tube Measurements*," [online database], Vols. 1–3, Mechanical Engineering Dept., Stanford Univ., Stanford, CA, http://hanson.stanford.edu/news.htm [retrieved 14 Oct. 2009].

[2] Davidson, D. F., and Hanson, R. K., "Interpreting Shock Tube Ignition Data," *International Journal of Chemical Kinetics*, Vol. 36, No. 9, 2004, pp. 510–523. doi:10.1002/kin.20024

[3] Sirjean, B., Dames, E., Sheen, D. A., You, X.-Q., Sung, C., Holley, A. T., Egolfopoulos, F. N., Wang, H., Vasu, S. S., Davidson, D. F., Hanson, R. K., Pitsch, H., Bowman, C. T., Kelley, A., Law, C. K., Tsang, W., Cernansky, N. P., Miller, D. L., Violi, A., and Lindstedt, R. P., "*A High-Temperature Chemical Kinetic Model of n-Alkane Oxidation: JetSurF, Version 0.2*," http://melchior.usc.edu/JetSurF/Version0_2/Index.html [retrieved 14 Oct. 2009].

[4] Westbrook, C. K., Pitz, W. J., Herbinet, O., Curran, H. J., and Silke, E. J., "A Detailed Chemical Kinetic Reaction Mechanism for *n*-Alkane Hydrocarbons from *n*-Octane to *n*-Hexadecane," *Combustion and Flame*, Vol. 156, No. 1, 2009, pp. 181–199. doi:10.1016/j.combustflame.2008.07.014

[5] Herbinet, O., Pitz, W. J., and Westbrook, C. K., "Detailed Chemical Kinetic Oxidation Mechanism for a Diodiesel Surrogate," *Combustion and Flame*, Vol. 154, No. 5, 2008, pp. 507–528. doi:10.1016/j.combustflame.2008.03.003

[6] Dooley, S., Curran, H. J., and Simmie, J. M., "Autoignition Measurements and a Validated Kinetic Model for the Biodiesel Surrogate, Methyl Butanoate," *Combustion and Flame*, Vol. 153, No. 1–2, 2008, pp. 2–32. doi:10.1016/j.combustflame.2008.01.005

[7] Horning, D. C., Davidson, D. F., and Hanson, R. K., "Study of the High-Temperature Autoignition of *n*-Alkane/O_2/Ar Mixtures," *Journal of Propulsion and Power*, Vol. 18, No. 2, 2002, pp. 363–371. doi:10.2514/2.5942

[8] Sato, K., and Hidaka, Y., "Shock-Tube and Modeling Study of Acetone Pyrolysis and Oxidation," *Combustion and Flame*, Vol. 122, No. 3, 2000, pp. 291–311. doi:10.1016/S0010-2180(00)00121-8

[9] Pichon, S., Black, G., Chaumeix, N., Yahyaoui, M., Curran, H. J., Simmie, J. M., and Donohue, R., "The Combustion Chemistry of a Fuel Tracer: Measured Flame Speeds and Ignition Delays and a Detailed Chemical Kinetic Model for the Oxidation of Acetone," *Combustion and Flame*, Vol. 156, No. 2, 2009, pp. 494–504. doi:10.1016/j.combustflame.2008.10.001

[10] Rothamer, D. A., Snyder, J. A., Hanson, R. K., Steeper, R. R., and Fitzgerald, R. P., "Simultaneous Imaging of Exhaust Gas Residuals and Temperature During HCCI Combustion," *Proceedings of the Combustion Institute*, Vol. 32, 2009, pp. 2869–2876. doi:10.1016/j.proci.2008.07.018

[11] Koch, J. D., and Hanson, R. K., "Temperature and Excitation Wavelength Dependencies of 3-Pentanone Absorption and Fluorescence for PLIF Applications," *Applied Physics B (Lasers and Optics)*, Vol. 76, No. 3, 2003, pp. 319–224. doi:10.1007/s00340-002-1084-4

[12] Farooq, A., Davidson, D. F., Hanson, R. K., Huynh, L. K., and Violi, A., "An Experimental and Computational Study of Methyl Ester Decomposition Pathways Using Shock Tubes," *Proceedings of the Combustion Institute*, Vol. 32, 2009, pp. 247–253. doi:10.1016/j.proci.2008.06.084

C. Avedisian
Associate Editor